Profiling the proteoforms of urinary prostate-specific antigen by capillary electrophoresis-mass spectrometry

Moran, A.B.; Dominguez Vega, E.; Nouta, J.; Pongracz, T.; Reijke, T.M. de; Wuhrer, M.; Lageveen-Kammeijer, G.S.M.

Journal of Proteomics 238 (2021) 104148

Contents lists available at ScienceDirect

Journal of Proteomics

journal homepage: www.elsevier.com/locate/jprot

Profiling the proteoforms of urinary prostate-specific antigen by capillary electrophoresis – mass spectrometry

Alan B. Moran [a], Elena Domínguez-Vega [a], Jan Nouta [a], Tamas Pongracz [a], Theo M. de Reijke [b], Manfred Wuhrer [a], Guinevere S.M. Lageveen-Kammeijer [a,*]

[a] Leiden University Medical Center, Center for Proteomics and Metabolomics, 2300 RC Leiden, the Netherlands
[b] Amsterdam UMC, location Academic Medical Center, Department of Urology, University of Amsterdam, Meibergdreef 9, 1105 AZ Amsterdam, the Netherlands

ARTICLE INFO

Keywords:
Prostate-specific antigen
Proteoforms
Intact protein analysis
Glycopeptide analysis
Capillary electrophoresis-electrospray ionization-mass spectrometry
Prostate cancer

ABSTRACT

Early detection of prostate cancer may lead to the overdiagnosis and overtreatment of patients as well as missing significant cancers. The current diagnostic approach uses elevated serum concentrations of prostate-specific antigen (PSA) as an indicator of risk. However, this test has been widely criticized as it shows poor specificity and sensitivity. In order to improve early detection and diagnosis, several studies have investigated whether different PSA proteoforms are correlated to prostate cancer. Until now, studies and methodologies for the comprehensive characterization of PSA proteoforms from biofluids are scarce. For this purpose, we developed an intact protein assay to analyze PSA by capillary electrophoresis-electrospray ionization-mass spectrometry after affinity purification from patients' urine. Here, we determined six proteolytic cleavage variants. In regard to glycosylation, tri-, di-, mono- and non-sialylated complex-type *N*-glycans were found on non-cleaved PSA, as well as the non-glycosylated variant. The performance of the intact protein assay was assessed using a pooled sample, obtaining an inter-day variability of 15%. Furthermore, urinary patient samples were analyzed by intact protein analysis and a bottom-up approach (glycopeptide analysis). This combined approach revealed complimentary information on both levels, demonstrating the benefit of using two orthogonal techniques to provide a thorough profile of urinary PSA.

Significance: The detection of clinically relevant prostate cancer requires a more specific and sensitive biomarker and, in this case, several PSA proteoforms may be able to aid or improve the current PSA test. However, a comprehensive analysis of the intact PSA proteoform profile is still lacking. This study investigated the PSA proteoforms present in urine and, in particular, determined the relative contribution of cleaved PSA and non-cleaved PSA forms to the total glycosylation profile. Importantly, intact protein analysis did not require further sample treatment before being measured by CE-ESI-MS. Furthermore, its glycosylation was also assessed in a bottom-up approach to provide complementary information. Overall, these results represent an important basis for future characterization and biomarker studies.

1. Introduction

An elevated serum level of prostate-specific antigen (PSA) was the first FDA approved tumor marker for the early detection of prostate cancer (PCa) [1,2]. However, since its approval, this serum-based test has come under increased scrutiny due to its lack of specificity and sensitivity [3]. For example, the test is unable to distinguish PCa from other prostate-related diseases, such as benign prostate hyperplasia (BPH) [1], as well as showing poor performance when differentiating aggressive from insignificant PCa. These issues are caused, in part, when the PSA concentration in serum is between 3 and 10 ng/mL (Netherlands [4]) or 4–10 ng/mL (United States [5]), the so-called diagnostic 'grey zone'. Patients with elevated serum PSA concentrations may undergo biopsy for further confirmation, however, only 26% of cases with PSA levels in the diagnostic grey zone have PCa [5]. Furthermore, the biopsy procedure is accompanied by risk factors such as infection and hematuria [5]. In general, patients risk being over- or under-treated and, therefore, would benefit greatly from more specific and sensitive biomarkers.

Several studies have investigated whether different PSA proteoforms

* Corresponding author.
E-mail address: g.s.m.kammeijer@lumc.nl (G.S.M. Lageveen-Kammeijer).

https://doi.org/10.1016/j.jprot.2021.104148
Received 29 October 2020; Received in revised form 26 January 2021; Accepted 31 January 2021
Available online 19 February 2021

might improve or aid the current PSA test [6,7]. In serum and seminal plasma, several naturally occurring PSA proteoforms are cleaved at specific internal cleavage sites (Fig. 1), resulting in enzymatically inactive variants [8–10]. A cleaved PSA form, containing a cleavage at Lys_{169} and Lys_{206}, is described as benign PSA (bPSA) due to its association with BPH [7]. Importantly, a feature of BPH is the overgrowth of cells located in the transition zone of the prostate [11], precisely the location where this cleavage is hypothesized to occur [7]. Conversely, in PCa, PSA circumvents this process when the epithelial lining becomes disrupted, resulting in the protein entering the bloodstream [12].

Investigations into PSA proteolytic cleavage variants have mainly been described in serum and seminal plasma; the proportion of cleaved PSA may account for 10 to 30% of total PSA in serum [13–15] whereas these proteoforms comprise 30% of PSA in seminal plasma [13,16]. However, another promising biofluid, urine, is relatively unexplored in this regard [17,18]. This is unfortunate since urine is likely to reflect the biological status of the prostate as there is evidence that PSA is directly secreted into urine via the periurethral glands [19,20]. Moreover, urine is relatively easy to obtain in high volumes with high concentrations of PSA [21,22]. In this case, an investigation into urinary PSA is warranted in order to define the specific proteoforms that are present there.

PSA glycosylation has been extensively studied as it has been reported to have potential diagnostic and prognostic value [18,23–25]. This protein contains a single *N*-glycosylation site present at Asn_{69}, normally containing complex-type di-sialylated and core-fucosylated glycans. A second *N*-glycosylation site might be present when Asp_{102} is replaced by Asn_{102} due to a mutation in the gene encoding PSA, kallikrein 3 (KLK3) [26], yet this has only been observed in a single study [27]. In general, PSA glycosylation in urine, seminal plasma and serum has been well examined [9,27–29]. Sarrats et al. demonstrated a similar glycosylation pattern between cleaved and non-cleaved PSA variants in seminal plasma and serum, respectively [29]. In contrast, small discrepancies were found when non-cleaved PSA glycopeptides were compared to the total PSA glycosylation profile [28]. Undoubtedly, the relative contribution of cleaved PSA forms to its total glycosylation is not well understood and requires further investigation.

Charge-based separation of PSA has previously been employed on the basis of the different isoelectric points (pIs) of its proteoforms [17,29]. For example, five distinct proteoforms were reliably separated using two-dimensional electrophoresis (2-DE) [29]. Here, however, only an estimated protein mass was determined using a molecular weight marker. Investigations that have applied mass spectrometry (MS) have provided a more accurate determination of the mass of PSA proteoforms [9]. In this case, separation was achieved using anion-exchange chromatography, although the proteoforms were analyzed offline by MS. Interestingly, capillary electrophoresis (CE) has been shown to be a suitable technique when hyphenated with electrospray ionization-MS (CE-ESI-MS) for online separation and identification of PSA proteoforms [30].

The main aim of this study was to investigate the profile of PSA proteoforms present in urine. For this purpose, PSA was captured from a patient urine pool and analyzed by CE-ESI-MS. In order to demonstrate the applicability of the protocol, the method was validated and further assessed using individual patient urine samples. Finally, an in-depth glycopeptide analysis was carried out to complement the glycosylation profile obtained at the intact protein level.

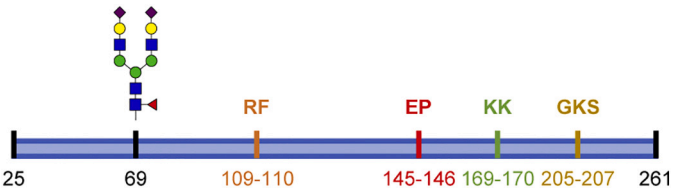

Fig. 1. *N*-glycosylation site and internal cleavage sites present in PSA. Amino acids are represented along the top whereas the sequence positions are represented along the bottom. Most abundant *N*-glycan (H5N4F1S2) is depicted on the *N*-glycosylation site (Asn_{69}). Fig. 1 adapted with permission [13] © (2003) American Society of Clinical Oncology. All rights reserved.

2. Materials and methods

2.1. Chemicals and reagents

Deionized water (MQ) was obtained with a Q-Gard 2 system (Millipore, Amsterdam, The Netherlands). Ammonium bicarbonate, potassium dihydrogen phosphate (KH_2PO_4), sodium bicarbonate ($NaHCO_3$), sodium chloride (NaCl), sodium hydroxide (NaOH), and sodium phosphate dibasic dihydrate ($Na_2HPO_4{\cdot}2H_2O$) were purchased from Merck (Darmstadt, Germany). Ammonium acetate, formic acid (FA), and water (LC-MS grade) were acquired from Fluka (Steinheim, Germany). Acetonitrile (LC-MS grade) was purchased from Biosolve (Valkenswaard, The Netherlands). Phosphate-buffered saline (PBS), five times concentrated (5×), was prepared from 0.16 M Na_2HPO_4, 0.02 M KH_2PO_4, 0.73 M NaCl at pH 7.2. 5× PBS was diluted with MQ to obtain 1× PBS, pH 7.6. DL-dithiothreitol (DTT), glacial acetic acid (HAc), hydrochloric acid (HCl), and iodoacetamide (IAA) were obtained from Sigma-Aldrich (Steinheim, Germany). Polyethylenimine (PEI) was obtained from Gelest (Morrisville, NC). Seminal PSA standard was acquired from Lee BioSolutions (St. Louis, MO). The protein test mixture, containing cytochrome C, lysozyme and ribonuclease A, was purchased from SCIEX (Brea, CA). Mass spectrometry-grade trypsin derived from bovine pancreas was purchased from Promega (Madison, WI). A synthetic peptide (LSEPAELTEAVK) was prepared in-house by FMoc solid phase peptide synthesis.

2.2. Sample collection

A waiver was obtained from the medical ethical committee (W16_010#16.020) of the Amsterdam University Medical Center (AMC) and clinical samples were collected over a two year period. Patients who were suspected of PCa and presented with an elevated PSA serum concentration (>3 ng/mL) donated urine prior to digital rectal examination (DRE) and prostate biopsy. Urinary samples were homogenized and portioned into BD Vacutainer™ Plastic Urinalysis Tubes (Fisher Scientific, Loughborough, UK). The samples were stored at −80 °C for a maximum of three months at the AMC before they were transferred to Leiden University Medical Center and stored at −80 °C. Sample processing was carried out at the end of the collection period.

2.3. Experimental design

2.3.1. Repeatability and intermediate precision assessment

In order to assess the repeatability and intermediate precision of the assay, an intra- and inter-day analysis was performed using a patient urine pool consisting of 27 patients (>180 mL), hereby referred to as the validation pool. This was divided into 20 mL portions and stored at −20 °C. Three full technical replicates were processed and measured each day ($n = 3$) over three days ($n = 9$). Urine was prepared as detailed in Sections 2.4–6.

2.3.2. Method application

The applicability of the protocol on individual patients was assessed using a separate cohort of patient samples ($n = 10$). Patient samples were randomized prior to sample treatment and 20 mL from each patient was processed over two batches. In addition, a positive control was created by pooling 5 mL from each of the 10 urine samples (50 mL) that was processed and measured in each batch. Urine was prepared according to Sections 2.4–6.

2.4. Sample processing

Urine was processed as previously described by Kammeijer et al. [28]. Briefly, samples were removed from storage, thawed at room temperature (RT) and vortexed to ensure a homogeneous mixture. Following this, the samples were centrifuged (500 *g*, 5 min) and 20 mL of urine supernatant was removed. The protocol has been validated to process 20 mL of urine and, therefore, in cases whereby urine was available below 20 mL, these samples were added up with 1× PBS to reach a total volume of 20 mL. Following this, 5 mL 5× PBS was added to all samples (final volume of 25 mL).

2.5. PSA capturing

PSA was isolated and immunopurified from urine as previously described [28]. Briefly, anti-PSA nanobodies (QVQ, Utrecht, The Netherlands) were coupled in-house with Sepharose beads (GE healthcare, Little Chalfont, UK). An overnight incubation at 4 °C was performed with the addition of 60 μL of a 50% anti-PSA beads solution to the samples. Next, the samples were centrifuged (100 *g*, 1 min), and the supernatant was removed to leave 500 μL of anti-PSA beads solution. This was followed by re-suspension and transfer to a 96-well polypropylene filter plate (Orochem, Naperville, IL), which was placed inside a vacuum manifold (Merck Millipore, Darmstadt, Germany). A vacuum was applied until there was no liquid remaining. Subsequently, the beads were washed with 600 μL 1× PBS followed by two washes using 600 μL of 50 mM ammonium bicarbonate. Following this, PSA was eluted using 200 μL of 100 mM FA containing a synthetic peptide (LSEPAELTEAVK; 45 fmol/μL). The plate was covered using an adhesive seal and placed on a plate shaker (max. rpm, 5 min). Finally, the plate was centrifuged (100 *g*, 2 min) and the eluent was split into two portions for intact protein analysis (80%) or enzymatic digestion with trypsin (20%) for glycopeptide analysis. Each portion was concentrated to dryness using a vacuum centrifuge operating at 45 °C (Eppendorf Concentrator 5301, Eppendorf). Samples were reconstituted in 3 μL of MQ (intact protein analysis) or 5 μL of 25 mM $NaHCO_3$ (glycopeptide analysis), and stored at −20 °C until further processing.

2.6. In-solution tryptic digestion

The portions set for glycopeptide analysis underwent reduction and alkylation prior to digestion with trypsin, as previously described [28]. Shortly, 1 μL of 12 mM DTT was added prior to incubation at 60 °C for 30 min. Further incubation was performed with 1 μL of 42 mM IAA for 30 min in darkness at RT. Finally, 1 μL of 48 mM DTT was added to the samples which remained in brightness for 20 min. Following this, 1 μL of 0.15 mg/mL trypsin was added in 25 mM $NaHCO_3$ and overnight digestion was performed at 37 °C.

2.7. Capillary electrophoresis

All experiments were performed on a CESI 8000 instrument (SCIEX) using bare-fused silica capillaries (91 cm × 30 μm i.d. × 150 μm o.d.) containing a porous tip. For intact protein analysis, capillaries were coated in-house using PEI and in accordance with a previously published protocol [31]. The temperature was set to 5 °C and 15 °C for the sample tray and capillary, respectively. The performance of the capillary was determined prior to performing measurements by assessing the migration time and signal intensity of a protein test mixture (SCIEX), as described previously [31]. When deemed necessary, the capillary coating was removed using 1 M NaOH (100 psi for 60 min) and re-coated according to the same procedure as mentioned above. In this case, however, no re-coating was required. Prior to analysis, the separation capillary was rinsed (100 psi for 5 min) with the background electrolyte (BGE) consisting of 20% HAc (*v/v*, 3.49 M, pH 2.3). Following this, the conductive line was filled with BGE (100 psi for 4 min) and hydrodynamic injection of the sample (8.8 psi for 35 s) was applied. Assuming a viscosity of aqueous BGE of 1.14 cP, 6.3% of the total capillary volume was filled (41 nL). The instrument was operated in reverse polarity mode and a separation voltage of 20 kV was applied for 45 min. The capillary was prevented from drying out between measurements by maintaining a constant low flow with the continuous application of 10 psi to the BGE vial.

Electrophoretic separation of glycopeptides was carried out in line with the protocol from literature [28]. Briefly, a bare-fused silica (BFS) capillary was flushed with 0.1 M NaOH (2.5 min), LC-MS grade H_2O (3 min), 0.1 M HCl (2.5 min), H_2O (3 min), followed by 3 min with the BGE of 20% HAc (*v/v*, 3.49 M, pH 2.3). Here, the sampling tray was set to 10 °C and the capillary temperature was maintained at 15 °C. The sample (4 μL) was mixed with 2 μL of leading electrolyte (1.2 M ammonium acetate, pH 3.17) in a PCR tube and subsequently transferred to nanovials (SCIEX, Brea, CA). Hydrodynamic injection of the sample was performed at 25 psi for 24 s (12.3% capillary volume / 79 nL). Following this, a BGE post plug was injected (0.5 psi for 25 s).

2.8. Mass spectrometry

On-line coupling of the CE system was achieved with a maXis Impact UHR-QqTOF (Ultra-High Resolution Qq-Time-Of-Flight) MS (Bruker Daltonics GmbH, Bremen, Germany) via a sheathless CE-ESI-MS interface and a nano-electrospray source. All MS experiments were performed in positive ionization mode and specific parameters were used for intact protein and glycopeptide analysis. For intact protein analysis, the following settings were used: electrospray voltage, 1350 V; nitrogen drying gas, 1.2 L/min at 100 °C; quadrupole ion energy, 5 eV; collision cell energy, 5 eV; transfer time, 120 μs; pre-pulse storage time, 20 μs. For glycopeptide analysis, the following parameters were implemented: electrospray voltage, 1100 V; nitrogen drying gas, 1.2 L/min at 150 °C; quadrupole ion energy, 3 eV; collision cell energy, 7 eV; transfer time, 130 μs; pre-pulse storage time, 15 μs. Furthermore, dopant enriched (ca. 4% mole percent acetonitrile) nitrogen (DEN)-gas was employed during glycopeptide analysis as previously described [32]. Briefly, the DEN-gas was introduced by allowing dry gas into a nanoBooster (OT3118G002, Bruker Daltonics); the coaxial sheath flow of the DEN-gas around the ESI emitter was introduced via an in-house made polymer cone, surrounding the housing of the porous tip. The MS data was acquired with a spectral acquisition frequency of 1 Hz within the range *m/z* 600–3000 or *m/z* 200–2200 for intact protein and glycopeptide analysis, respectively.

2.9. Data analysis

Bruker DataAnalysis version 5.0 was used to perform data analysis. For assignments of intact proteoforms, internal calibration was carried out using the top 10 charge states ($[M + 13H]^{13+} - [M + 22H]^{22+}$) of the most abundant peak in combination with $[M + 1H]^{1+}$ and $[M + 2H]^{2+}$ of a synthetic peptide (LSEPAELTEAVK) as calibration points. Then, the spectra of interest were averaged, smoothed (Gaussian, 0.05 Da) and deconvoluted. Mass spectra deconvolution was performed using the maximum entropy algorithm. Data point spacing and instrument resolving power were set to *m/z* 0.5 and 10^4 FWHM, respectively. Assignments of the peaks were made by employing a tolerance of ≤25 ppm. Theoretical *m/z* values were generated for assigned peaks using an in-house developed software (LaCyTools, version 1.1) [33]. Extracted ion electropherograms (EIEs) were generated using the three most abundant charge states of assigned peaks with an extraction window of ± *m/z* 0.1. Electropherogram smoothing was applied to all EIEs (Gaussian, 2.0 points). Following this, peak areas were obtained via manual integration.

For glycopeptides, EIEs were created using the first three isotopes across three charge states ($[M + H]^{+} - [M + 3H]^{3+}$) with an extraction window of ± *m/z* 0.05. Glycopeptide structures, including differently linked sialic acid isomers, were assigned based on a mass tolerance of

≤10 ppm and previously published research [28]. Glycoforms were labeled as glycan net compositions that specifies number of hexoses (H), *N*-acetylglucosamines (N), fucoses (F) and *N*-acetyl neuraminic acids (S); these monosaccharide abbreviations will be further used throughout this manuscript. EIE areas were obtained via manual integration and adjusted to represent the entire isotopic envelope.

3. Results

3.1. Intact urinary PSA

3.1.1. PSA proteoform analysis by CE-ESI-MS

Separation for intact protein analysis with CE-ESI-MS was optimized using a seminal PSA standard, as summarized in Supporting Information, Table S-1. Briefly, the capillary was positively coated using PEI, a polymer which has been reported to reduce protein-capillary inner surface interactions [31]. The capillary was operated at 20 kV in reverse polarity mode in order for the electroosmotic flow to migrate towards the capillary outlet and the MS inlet. Separation of proteoforms was achieved by using 20% HAc as the BGE and the separation between the sialylated and non-sialylated glycoforms was increased by lowering the capillary temperature to 15 °C. Capturing and purification was performed as previously described with no amendments to the original procedure [28] and PSA from urine was directly analyzed by CE-ESI-MS.

The analysis of intact PSA from the validation pool revealed a number of different proteoforms; six proteolytic cleavage variants, which included cleaved and non-cleaved forms, as well as a variation in the composition of glycan structures attached to the protein (Fig. 2). The tentative assignment of cleavage sites is demonstrated in Fig. 3. A single cleavage, due to hydrolysis of the peptide bond between two amino acids at a cleavage site, is indicated by an 18 Da increase of the intact protein mass caused by the incorporation of a water molecule. Despite this cleavage, disulfide bridges keep the protein chains covalently connected. In the instance of a protein with a double cleavage, two peptide bonds undergo hydrolysis at two cleavage sites, respectively. This is indicated by a 36 Da increment of the protein mass due to the addition of a water molecule at each cleavage site. Importantly, specific cleavage sites could be indicated when apparent losses of adjacent amino acids were observed at the well-known cleavage sites (Arg_{109}Phe, Glu_{145}Pro, Lys_{169}Lys, $Gly_{205}Lys_{206}$Ser) [9].

As illustrated in Fig. 2, the double cleaved variant migrated first followed by the single cleaved and eventually the non-cleaved variants. Here, the most abundant glycoprotein present per proteoform is shown. The main form of PSA with two cleavages was assigned to a cleavage at position Glu_{145}, due to the loss of Glu, whereas the second cleavage site remained unidentified, as only a second hydrolysis was indicated by an 18 Da increase of the intact protein mass and no amino acid loss was observed. The single cleavage sites were determined at Arg_{109} and Lys_{206} due to a single hydrolysis and loss of the adjacent amino acids there. Another single cleavage at Lys_{169}/Lys_{206} could not be further specified as loss of a lysine residue is possible at both sites. One variant migrating at 21.2 mins (Fig. 2B) could not be assigned to a specific site as only a single hydrolysis was observed and no loss of an amino acid was detected. For non-cleaved PSA, the most abundant glycoforms on this proteoform are shown in Fig. 2C. Here, the glycoforms with the highest number of sialic acids migrate first and the non-sialylated glycoforms

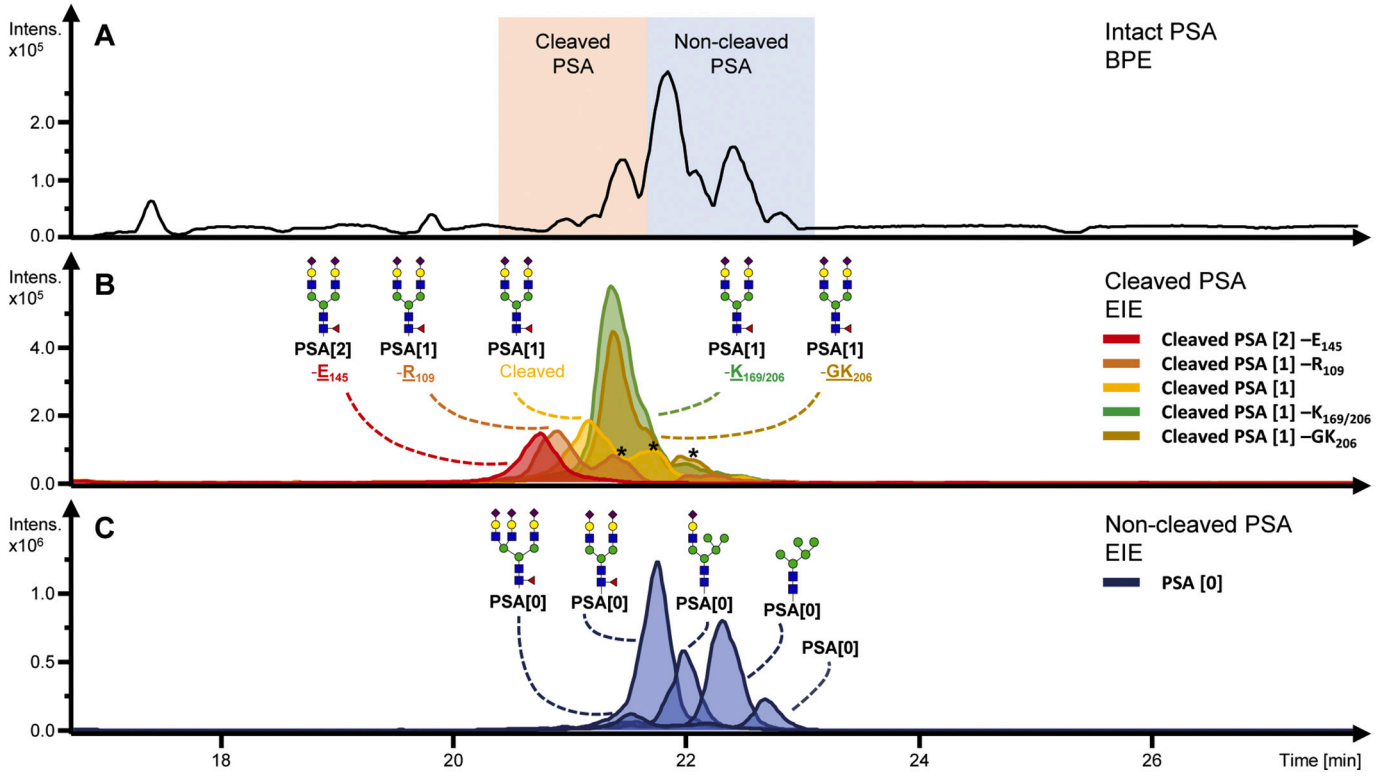

Fig. 2. Intact protein analysis using CE-ESI-MS of PSA captured from a patient urinary pool. (A) Base peak electropherogram (BPE) of intact urinary PSA. A variation in PSA proteoforms can be observed with and without internal cleavages. (B) The EIEs illustrate the most abundant glycoprotein present per proteoform. Proteoforms with different numbers of internal cleavages can be observed with the number of internal cleavages indicated in the square brackets: PSA[2] -E_{145}, double cleaved PSA at E_{145} and one other unidentified position; PSA[1] -R_{109}, cleaved PSA at R_{109}; PSA[1] -Cleaved, cleaved PSA at a unidentified position; PSA[1] -$K_{169/206}$, cleaved PSA at either K_{169} or K_{206}; PSA[1] -GK_{206}, cleaved PSA at GK_{206} (C) For non-cleaved PSA the most abundant tri-, di- and mono-sialyated form is illustrated as well as the most abundant high mannose type and the non-glycosylated form of the protein. Asterisk (*) indicates overlapping *m/z* values in different electrophoretic peaks. Blue square: *N*-acetylglucosamine, green circle: mannose, yellow circle: galactose, red triangle: fucose, pink diamond: *N*-acetylneuraminic acid. (For interpretation of the references to colour in this figure legend, the reader is referred to the web version of this article.)

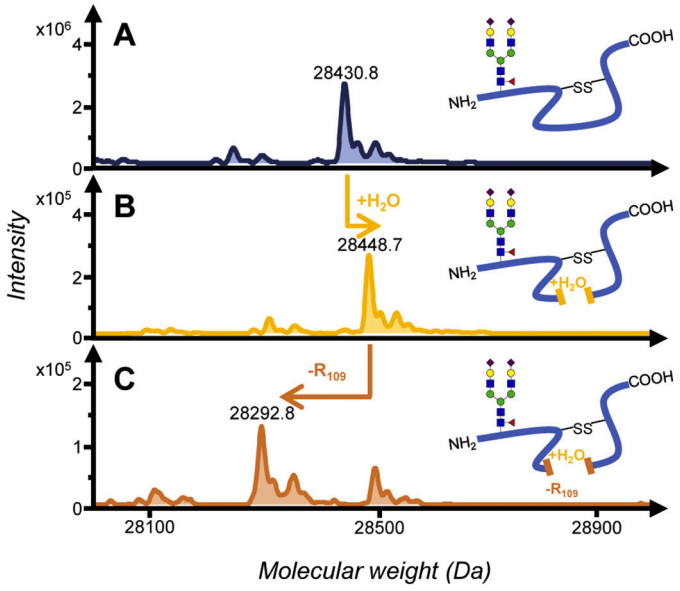

Fig. 3. Assignment of proteolytic cleavage variants based on amino acid loss at the cleavage site. (A) Deconvoluted mass spectrum of non-cleaved PSA accompanied by a graphical representation (right) of the protein and the most abundant *N*-glycan. (B) Hydrolysis of the peptide bond at an unidentified cleavage site increases the mass (18 Da) of the protein. The protein is inactivated due to this internal cleavage, however the structure remains intact as a result of disulfide bridges at the cysteine residues. (C) The internal cleavage site may be determined, in accordance with literature [9], whereby hydrolysis of the peptide bond and loss of an amino acid at the cleavage site occurs. Blue square: *N*-acetylglucosamine, green circle: mannose, yellow circle: galactose, red triangle: fucose, pink diamond: *N*-acetylneuraminic acid. (For interpretation of the references to colour in this figure legend, the reader is referred to the web version of this article.)

migrated latest, followed by the non-glycosylated protein. Interestingly, the di-sialylated *N*-glycan structure, H5N4F1S2, was the dominant glycoform for all cleaved and non-cleaved PSA variants (Fig. 2 and Supporting Information, Table S-2). Overall, intact protein analysis revealed that PSA consists of a complex array of proteoforms, including cleaved and non-cleaved forms, as well as a high variation in glycosylation.

3.1.2. Repeatability and intermediate precision

In order to validate and assess the applicability of the complete intact protein assay for the analysis of biological samples, the repeatability and intermediate precision was established via intra- ($n = 3$) and inter-day ($n = 3$) measurements (total $n = 9$). The data processing protocol was also optimized by testing a number of data extraction parameters as summarized in Supporting Information, Table S-1. Similar results were obtained for the quantification via deconvolution or EIEs. Thus, it was decided to perform the quantification using EIEs, using the three most abundant charge states, as the Bruker Data Analysis software is more suited for this purpose. In addition, an extraction window of ± *m/z* 0.1 was used because it allowed the least overlap with other masses while maintaining the highest sensitivity. Various methods of internal calibration were tested, including internal calibration based only on the charge envelope of H5N4F1S2, or internal calibration using a combination of H5N4F1S2 and a synthetic peptide (LSEPAELTEAVK). The former method only covers *m/z* 1200–2200, whereas the latter method covers a larger range of *m/z* ratios (*m/z* 650–2200) and was eventually selected for further processing. In total, 32 proteoforms (≤25 ppm) were identified in the validation pool, including six proteolytic cleavage variants and 21 *N*-glycan structures (Fig. 4 and Supporting Information, Table S-2). In the end, an average *coefficient of variation* (CV) of 11% and 15%, including all 32 proteoforms, was found for the intra-day and inter-day analysis, respectively. The CVs shown here represent the full

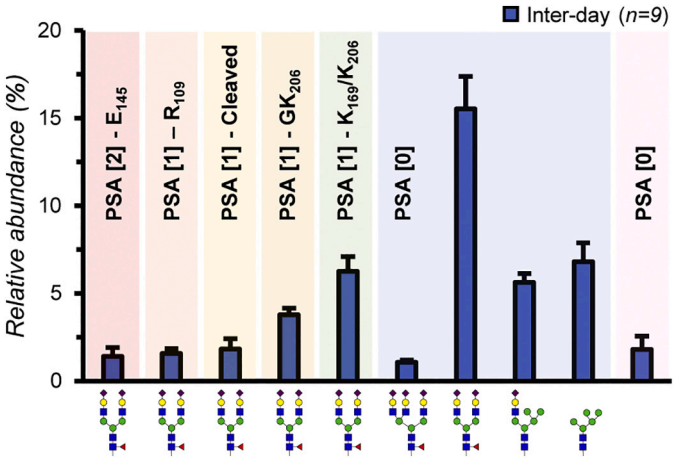

Fig. 4. Intermediate precision and repeatability of intact PSA assay measured by CE-ESI-MS. Inter-day relative areas (%) are shown for the most abundant glycoprotein present per proteoform (normalized to the sum area of all assigned glycoprotein forms). Each bar represents the mean and the standard deviation ($n = 9$) is represented by the error bars. Background colours denote different internal cleavage sites: the square brackets denote the number of cleavages present in that proteoform. The site of internal cleavage, in accordance with the literature [9] and observed amino acid loss, is illustrated using the position within the amino acid sequence. In green, internal cleavage may occur at either K_{169} or K_{206}. Blue square: *N*-acetylglucosamine, green circle: mannose, yellow circle: galactose, red triangle: fucose, pink diamond: *N*-acetylneuraminic acid. (For interpretation of the references to colour in this figure legend, the reader is referred to the web version of this article.)

assay performance, demonstrating the entire variation introduced from the capture procedure, the CE-ESI-MS measurement up to the manual data processing step.

3.1.3. Assessment of PSA proteoforms from patient urine

The presence and abundance of PSA proteoforms in biological samples (urine) was assessed using a small cohort of patients' urine samples ($n = 10$). Eight patients provided a detectable signal for the intact protein analysis of urinary PSA; diagnoses for these patients was provided after completion of the measurement and data processing, resulting in a cohort of five non-PCa and three PCa patients. During the intra- and inter-day assessment, 32 proteoforms were identified. From this, 23 out of the 32 could be observed in the positive control with ppm errors ≤25 (Fig. 5 and Supporting Information, Fig. S-1 and Table S-3). In all samples the relative abundance of di-sialylated glycoforms was assessed on cleaved and non-cleaved PSA. No major differences were detected in the relative abundances of di-sialylated glycoforms present on the most abundant form of cleaved PSA, Lys_{169}/Lys_{206}, in comparison with non-cleaved PSA (Fig. 6). Additionally, one patient (patient E) showed evidence of having an extra *N*-glycosylation site, as a result of the conversion of Asp_{102} to Asn_{102}, which was populated mainly with high-mannose type glycans (Supporting Information, Table S-3). Similar relative abundances were found for the positive control ($n = 2$; Fig. 5), which suggests that little bias was introduced into the analysis as a result of batch processing. Furthermore, the performance of the assay, as indicated by the positive control, is consistent with the performance previously validated by the intra- and inter-day study. Finally, an average CV of 48% ($n = 8$) was found for the 10 most abundant proteoforms, which should represent the broad biological variation present within the entire cohort.

3.2. Intact protein and glycopeptide comparison

In order to support and expand the glycoform assignment performed at the intact protein level, the patient samples were additionally

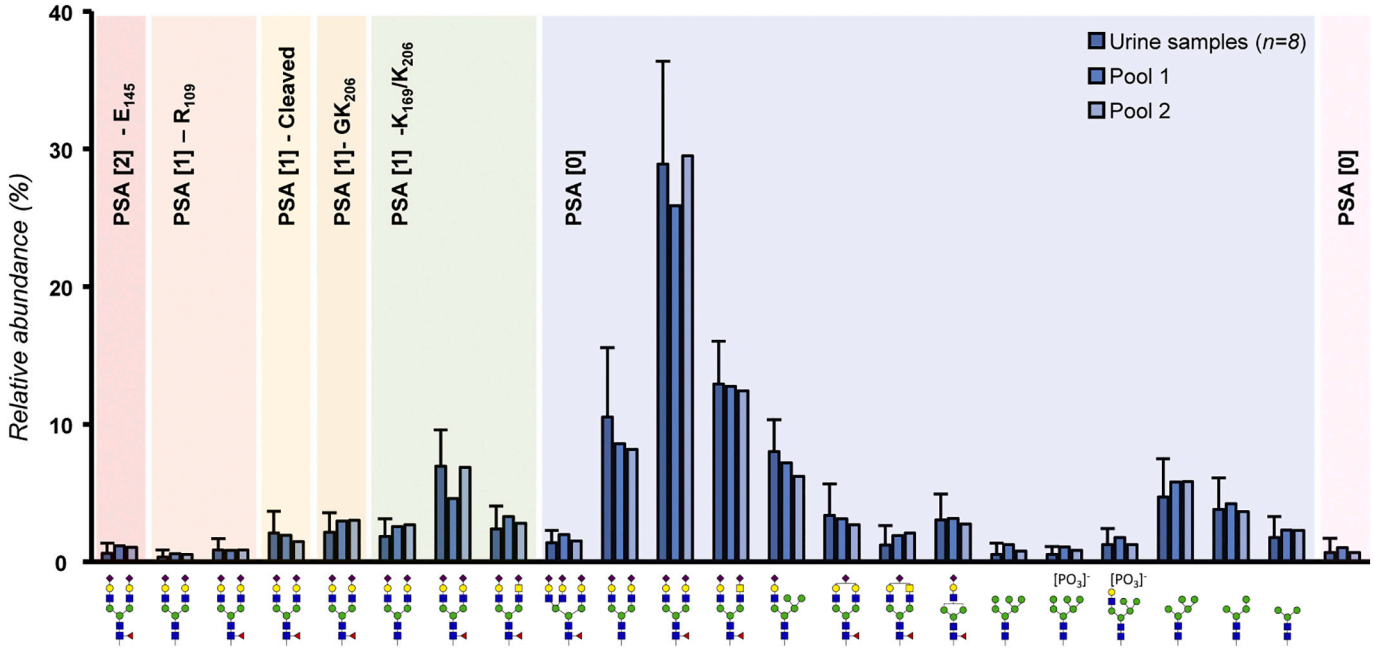

Fig. 5. Intact protein assay for the analysis of patient urinary PSA with CE-ESI-MS. All 23 identified proteoforms (ppm error ≤ 25) are represented as a relative (%) area (normalized to the sum of all 23 glycoprotein forms). A single bar represents the mean of patients' urine samples measurements ($n = 8$), whereas both pools are shown, representing the positive control of each batch. The error bars represent the biological variation amongst the urine samples. Colours denote the different proteolytic cleavage variants of PSA; square brackets denote the number of cleavages present in that proteoform. The site of internal cleavage, in accordance with literature [9] and observed amino acid loss, is illustrated using the position within the amino acid sequence. Blue square: *N*-acetylglucosamine, green circle: mannose, yellow circle: galactose, red triangle: fucose, pink diamond: *N*-acetylneuraminic acid. (For interpretation of the references to colour in this figure legend, the reader is referred to the web version of this article.)

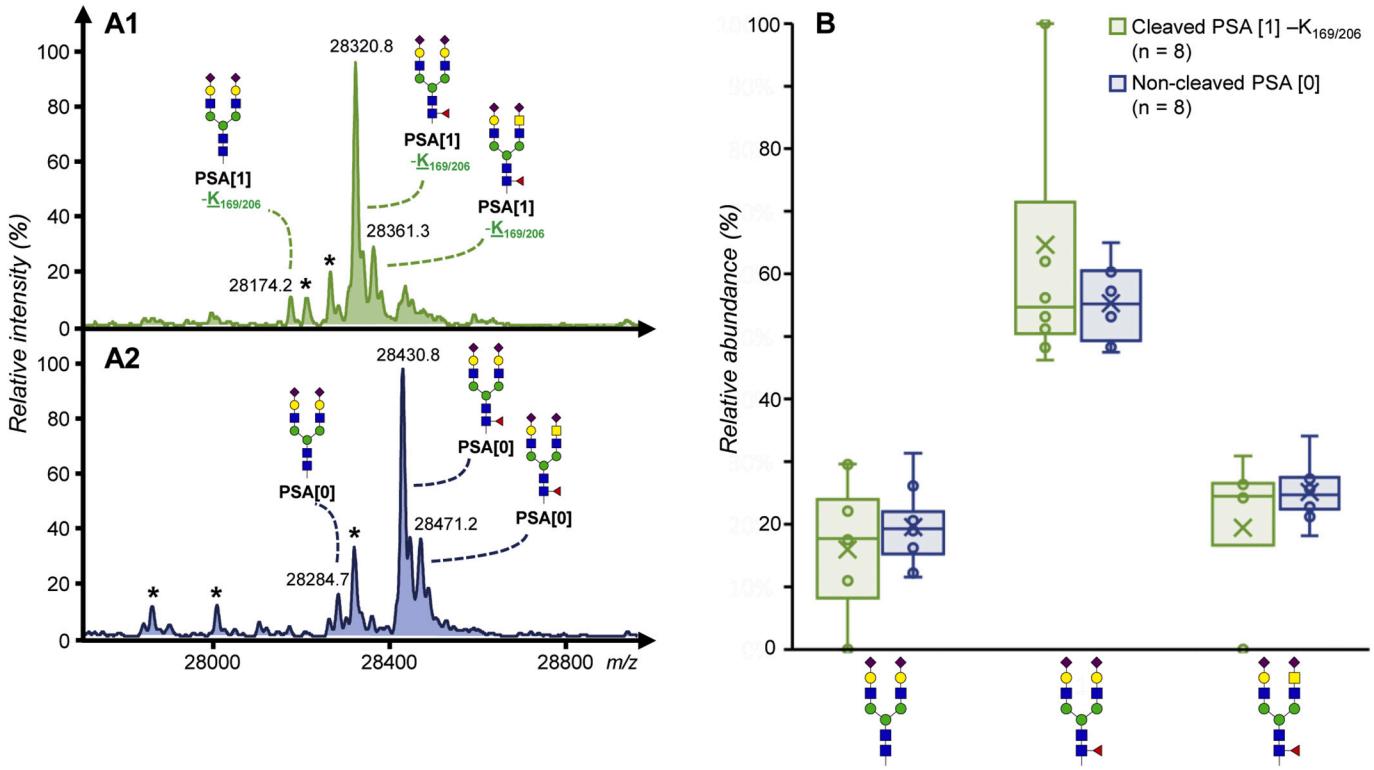

Fig. 6. Relative abundances of di-sialylated glycans on cleaved PSA -$K_{169/206}$ and non-cleaved PSA. (A) Representative deconvoluted mass spectra of intact urinary PSA of (A1) cleaved PSA -$K_{169/206}$ that contains the same di-sialylated complex glycans as (A2) non-cleaved PSA. Asterisk (*) indicates overlapping proteoforms in different electrophoretic peaks. (B) Relative abundance of H5N4S2, H5N4F1S2, and H4N5F1S2 (normalized to all 3 di-sialylated structures) in cleaved PSA -$K_{169/206}$ and non-cleaved PSA in the urine samples ($n = 8$). Blue square: *N*-acetylglucosamine, green circle: mannose, yellow circle: galactose, red triangle: fucose, pink diamond: *N*-acetylneuraminic acid. (For interpretation of the references to colour in this figure legend, the reader is referred to the web version of this article.)

analyzed by glycopeptide analysis. Importantly, the entire sample preparation was performed within the same protocol. Glycopeptide analysis detected glycoforms in all urine samples ($n = 10$), whereas the intact protein approach only detected proteolytic cleavage variants and glycoforms in some ($n = 8$). In total, 12 glycoforms could be identified by both intact protein and glycopeptide analysis (Fig. 7A and Supporting Information, Table S-4). To test the correlation between both approaches, the variation in the most abundant glycoform, H5N4F1S2, was examined (normalized to the sum of the six most abundant glycoforms; Fig. 7B). An association of $R^2 = 0.86$ was found. Furthermore, glycopeptide analysis identified an additional 63 structures, whilst intact protein analysis detected two structures (H6N2 and H3N2) that were not detected during glycopeptide analysis (Supporting Information, Table S-3). The identities of the two most abundant glycans present at the extra *N*-glycosylation site in patient E (H5N2 and H6N2) were confirmed by glycopeptide analysis. In total, the combined PSA analysis was able to identify 77 *N*-glycans, as well as two extra *N*-glycans on Asn_{102}, and six proteolytic cleavage variants.

4. Discussion

Many proteoforms of the glycoprotein PSA are related to PCa or other prostate-related diseases, including cleaved and precursor forms, as well as aberrant glycosylation [6,7,24]. PSA proteoforms have been described in serum and seminal plasma, yet urinary PSA remains poorly understood in this sense. Thus, in order to assess the broad range of PSA proteoforms present in urine, we established and validated an intact protein assay for the analysis of urinary PSA.

4.1. Proteoform analysis by CE-ESI-MS

As illustrated by Fig. 2, PSA proteoforms display a predictable migration pattern caused most likely by their different hydrodynamic volume and pI [16]. In previous studies, the pI of PSA proteoforms, such as non-glycosylated PSA (7.2) and di-sialylated PSA (6.8), was examined using two-dimensional electrophoresis [29]. However, *N*-glycan analysis revealed the same glycosylation pattern for di-sialylated PSA and proteoforms with lower pIs. Therefore, the difference in pIs cannot be attributed to sialylation and is likely due to different proteolytic cleavage variants [29]. Similarly, we observed the separation of these forms mainly due to proteolytic cleavages and the resulting loss of polar amino acids (Glu, Arg and Lys) [17,34]. The cleavages at Arg_{109}, Glu_{145}, Lys_{169}/Lys_{206}, and $Gly_{205}Lys_{206}$, as determined by the loss of these amino acids and their corresponding mass, are in line with cleavage sites detected on PSA in seminal plasma and serum [9,35]. Cleavage at Lys_{206} is associated with the formation of bPSA, although Mikolajczyk et al. originally described bPSA as a double cleavage variant with cleavages at Lys_{169} and Lys_{206} [7]. However, we did not detect this particular double cleavage variant during this study.

Despite this, bPSA has generally been characterized by SDS-PAGE following isolation using chromatographic based methods, which were unable to separate distinct cleaved PSA forms [7,36]. In addition, bPSA has been described as several cleaved PSA forms in the literature [13,37]. Thus, it is apparent that cleaved PSA requires further characterization as, for example, it is unclear whether bPSA consistently features cleavages at Lys_{169} and Lys_{206}, or whether other PSA cleavages are likewise associated with the development of BPH. While our study already provides more confidence for the assignment of the PSA proteolytic cleaved variants, compared to assignments based upon SDS-PAGE, further studies are needed to obtain an even more detailed structural characterization (e.g. MS/MS) of the wide range of proteolytic cleaved variants.

PSA is secreted by the prostate and internal cleavage is thought to occur post-translationally by proteases in hyperplastic prostate tissue [38]. In contrast, glycosylation occurs intracellularly where it may be disrupted due to cancer-associated changes to the cell glycosylation

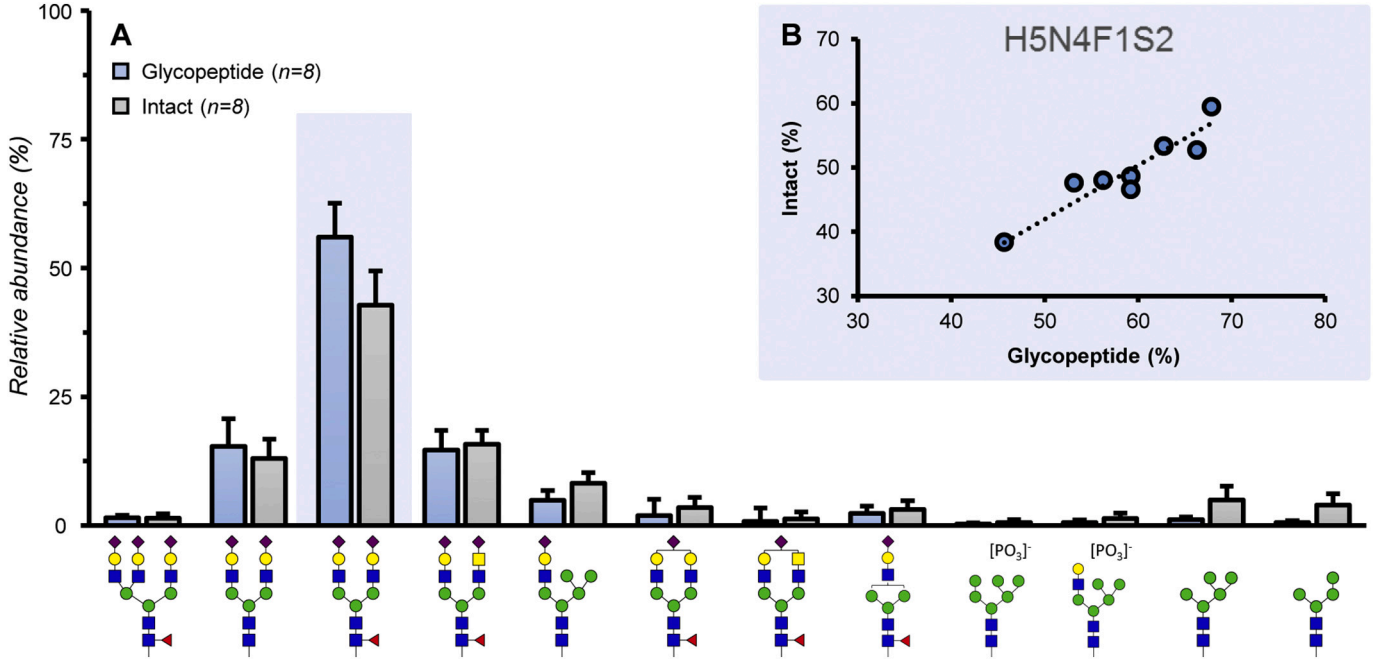

Fig. 7. Comparison of the intact protein and glycopeptide approaches for glycosylation quantification of urinary PSA from patients. (A) All glycoforms detected across different cleaved and non-cleaved PSA forms were determined as a single glycoform for the purpose of comparing glycosylation profiles between intact and glycopeptide. In both cases, only glycoforms detected in both the intact protein and glycopeptide datasets (12) were used to calculate the relative abundances (normalized to all 12 glycoforms). Each bar represents the mean of patients' urine samples measurements ($n = 8$) in both datasets, while error bars represent the standard deviation. (B) Relative abundance of H5N4F1S2 (normalized to top six most abundant glycoforms: H5N4S2, H5N4F1S2, H4N5F1S2, H6N3S1, H5N4F1S1, H4N3F1S1) detected in the glycopeptide patient dataset (x-axis) against the same glycoform detected during intact protein analysis of patients (y-axis). Equation of the regression line: $y = 0.8387\times$, $R^2 = 0.8648$. Blue square: *N*-acetylglucosamine, green circle: mannose, yellow circle: galactose, red triangle: fucose, pink diamond: *N*-acetylneuraminic acid. (For interpretation of the references to colour in this figure legend, the reader is referred to the web version of this article.)

machinery [39]. Although it is unclear whether protein glycosylation undergoes further matrix-associated modifications, it is unlikely that these processes are specifically related to the internal cleavage of PSA. This view is supported by the present study as the same di-sialylated species were detected both on cleaved and non-cleaved PSA (Fig. 4). Furthermore, a similar relative abundance of these structures is detected in urine across various patients (Fig. 6 and Supporting Information, Fig. S-2). As a result, it seems that the cleavage of PSA is independent of the glycosylation. Similarly, di-sialylated complex-type *N*-glycans have consistently been described as the main glycoform across cleaved PSA variants in seminal plasma and serum [9,29,40]. Presumably, glycan species that are less abundant are also present on cleaved PSA, yet have not been detected thus far and such an in-depth investigation is warranted in order to fully explore the glycan diversity of cleaved PSA.

4.2. Intact data processing and quantification

This method has demonstrated a similar performance to analyses that are more commonly performed with biopharmaceuticals. The intra- (11%) and inter-day (15%) CVs reported here are comparable with those described for the intact protein analysis of recombinant gonadotropin (≤10%) [41] and antibody-derived therapeutics (8–11%) [42]. Naturally, the analysis of standardized products represents only the measurement variation whereas analysis of clinical samples also includes error prone steps such as protein capturing and purification. Furthermore, the relative quantification of intact PSA proteoforms applied here is useful in this setting as the relative increase or decrease of specific proteoforms is likely to represent biological changes related to prostate disease.

The platform, however, is limited by data processing, which represents an analytical bottleneck for the investigation of clinical cohorts. Multiple protocols are presented in the literature with little consensus [43]. In this study, several data integration techniques were tested (Supporting Information, Table S-1) and our findings revealed that integrating the EIE area, generated by the average mass of the three most abundant charge states per proteoform, provided reliable results in a reasonably time-efficient manner. Similar results and parameters have been reported previously, whereby quantification of intact proteins was performed using EIEs [44]. However, overlap of m/z signals causes broad and sometimes numerous EIE peaks. As a result, manual peak integration is required which greatly increases the processing time per sample. Additionally, the issue is further compounded by the lack of dedicated software [43]. Therefore, data processing presents the major bottleneck for the application of this method to larger clinical cohorts. In the case of PSA, cleaved and non-cleaved variants may be reliably separated and it seems that the expression and level of glycosylation is similar between these forms. Thus, future investigations could focus solely on cleaved PSA by performing *N*-glycan release prior to performing the intact protein measurement. This would reduce the complexity of the analysis whilst maintaining important information regarding the proteolytic cleavage variants.

4.3. Glycosylation quantification

The glycopeptide approach revealed 40 unique *N*-glycan compositions, or 75 structures in total including sialic acid isomers. Linkage determination of sialic acids is a crucial aspect as α2,3-sialylated PSA has been shown to differentiate PCa from non-PCa patients [24]. However, the intact protein approach was unable to determine differently linked sialylated PSA, and only a limited set of 12 glycoforms was covered by both methods, nonetheless, similar relative abundances were observed (Fig. 7). Accordingly, relative quantification of H5N4F1S2 in the patient urine samples showed good correlation for the two approaches. However, some disparity was found in the relative quantification of the glycoforms H4N2 and H5N2. Moreover, the glycoforms, H6N2 and H3N2 were detected at the intact protein level but were not observed by the glycopeptide approach. This disparity in high-mannose form quantification might be related to their low abundance as the quantification of minor forms is often inconsistent for both approaches. Furthermore, different ionization efficiencies between mannose and sialylated species might also contribute to different relative quantification results by both techniques. Nonetheless, it remains unclear why specific high-mannose forms could not be detected during glycopeptide analysis and further research will be needed to determine whether this is a limitation of the method.

4.4. Complementary intact protein and glycopeptide analysis

The glycopeptide approach, as described above, demonstrates advantages in sialic acid linkage determination and overall higher sensitivity as illustrated by the number of glycoforms detected. This is achieved as the same dipeptide backbone ($Asn_{69}Lys$) is observed for cleaved and non-cleaved PSA after proteolytic digestion by trypsin, and represents a summed glycosylation profile of all proteoforms. However, specificity in relation to each proteolytic cleavage variant is lost. This is in contrast with the intact protein analysis, where six distinct proteolytic cleavage variants were detected, including non-glycosylated PSA for which the peptide is too small to be assessed by CE-ESI-MS. In addition, the intact protein analysis was able to determine the most abundant glycoforms per proteolytic cleavage variant (Fig. 6 and Supporting Information, Fig. S-2). One of the most interesting findings was the presence of an extra *N*-glycosylation site on PSA of patient E which could be confirmed by the glycopeptide approach (Supporting Information, Table S-5). The identification in the glycopeptide approach had initially been hampered due to the co-migration of more intense tryptic peptide peaks (Supporting Information, Fig. S-3). As in agreement with the intact protein analysis, high-mannose type glycans H5N2 and H6N2 were detected as the two most abundant glycans present at this site and the non-glycosylated variant was also not observed. Interestingly, the second *N*-glycosylation site has only been described in one other study, of which the reports of high-mannose structures are consistent [27]. Overall, this study demonstrates the complementarity between the two different approaches, which together form a highly suitable platform to study the proteolytic cleaved PSA variants, non-cleaved PSA and its glycosylation as each is required in order to perform full characterization of PSA, and in some cases, may be used to crosscheck results.

4.5. Perspectives

Urine, serum and seminal plasma represent different biological reservoirs of PSA [12,21,45], and PSA analysis from each of these biofluids comes with specific challenges as well as advantages for clinical use. During this study, the main focus was on urinary PSA, yet PSA proteoforms in other biofluids, particularly serum, also lack such an in-depth analysis. In order to apply the established assay to serum PSA, further development would be required as serum PSA is generally 5 to 50-fold lower in concentration compared to urine [21]. For this purpose, it would be necessary to improve the sensitivity, capturing efficiency and detection of the assay. Furthermore, during this study, some patients revealed urinary PSA concentrations that were too low for intact protein analysis, therefore the analysis of urine following DRE might be more suitable as it would be expected to have a higher concentration of PSA [46]. Finally, improvements to intact protein sample and data throughput would be needed in order obtain statistically significant results from a larger clinical cohort. Nevertheless, further exploration of PSA from urine, serum and seminal plasma should be continued as it represents a rich source of potential informative and non-invasive biomarkers for prostate cancer.

5. Conclusions

In this study, we validated an intact protein assay for the

determination of PSA proteoforms. The assay was applied to a small cohort of patients, in which six different proteolytic cleavage variants were detected. The proteolytic cleavage variants included double and single cleaved forms and non-cleaved forms of PSA that have also been described in seminal plasma and serum. Additionally, cleaved PSA showed a similar relative abundance of glycoforms as non-cleaved PSA. Glycosylation profiles obtained at the intact protein level were confirmed using the more in-depth glycopeptide approach, and both approaches in combination determined a second *N*-linked glycosylation site of PSA in one patient. Finally, it was illustrated that the developed protocol is able to assess cleaved PSA (intact protein analysis) and glycosylation (glycopeptide analysis) of individual patients in the same procedure, revealing the benefit of adding the intact protein level to the bottom-up approach.

6. Data availability

The raw mass spectrometric data files that support the findings of this study are available in the MassIVE repository and may be found with the data set identifier MSV000086699 https://doi.org/10.25345/C5HF79 [47].

Funding

This research was supported by the Marie Skłodowska-Curie actions as part of European Union's Horizon 2020 Research and Innovation Program (GlySign, Grant No. 722095), Cure for Cancer Foundation, Astellas Pharma B.V and SCIEX. The authors declare no competing financial interest.

Acknowledgements

We thank Sarah Azaabal and for her early work on the intact protein CE-ESI-MS method. We would also like to thank Bas C. Jansen for his valuable guidance on using LaCyTools.

Appendix A. Supplementary data

Supplementary data to this article can be found online at https://doi.org/10.1016/j.jprot.2021.104148.

References

[1] G. De Angelis, H.G. Rittenhouse, S.D. Mikolajczyk, L. Blair Shamel, A. Semjonow, Twenty years of PSA: from prostate antigen to tumor marker, Rev. Urol. (2007) 113–123.
[2] C. Kouriefs, M. Sahoyl, P. Grange, G. Muir, Prostate specific antigen through the years, Arch. Ital. Urol. Androl. (2009) 195–198.
[3] V.A. Moyer, U.S. Preventive Services Task Force, screening for prostate cancer: US Preventive Services Task Force Recommendation Statement, Ann. Intern. Med. 157 (2) (2012) 120.
[4] F.H. Schroder, J. Hugosson, M.J. Roobol, T.L. Tammela, M. Zappa, V. Nelen, M. Kwiatkowski, M. Lujan, L. Maattanen, H. Lilja, L.J. Denis, F. Recker, A. Paez, C. H. Bangma, S. Carlsson, D. Puliti, A. Villers, X. Rebillard, M. Hakama, U. H. Stenman, P. Kujala, K. Taari, G. Aus, A. Huber, T.H. van der Kwast, R.H. van Schaik, H.J. de Koning, S.M. Moss, A. Auvinen, E. Investigators, Screening and prostate cancer mortality: results of the European Randomised Study of Screening for Prostate Cancer (ERSPC) at 13 years of follow-up, Lancet 384 (9959) (2014) 2027–2035.
[5] T. Ross, K. Ahmed, N. Raison, B. Challacombe, P. Dasgupta, Clarifying the PSA grey zone: the management of patients with a borderline PSA, Int. J. Clin. Pract. 70 (11) (2016) 950–959.
[6] S.D. Mikolajczyk, L.S. Millar, T.J. Wang, H.G. Rittenhouse, L.S. Marks, W. Song, T. M. Wheeler, K.M. Slawin, A precursor form of prostate-specific antigen is more highly elevated in prostate cancer compared with benign transition zone prostate tissue, Cancer Res. (2000) 756–759.
[7] S.D. Mikolajczyk, L.S. Millar, T.J. Wang, H.G. Rittenhouse, R.L. Wolfert, L.S. Marks, W. Song, T.M. Wheeler, K.M. Slawin, "BPSA," a specific molecular form of free prostate-specific antigen, is found predominantly in the transition zone of patients with nodular benign prostatic hyperplasia, Urology 55 (1) (2000) 41–45.
[8] K.W. Watt, P.J. Lee, T. M'Timkulu, W.P. Chan, R. Loor, Human prostate-specific antigen: structural and functional similarity with serine proteases, Proc. Natl. Acad. Sci. U. S. A. 83 (10) (1986) 3166–3170.
[9] J.M. Mattsson, L. Valmu, P. Laakkonen, U.H. Stenman, H. Koistinen, Structural characterization and anti-angiogenic properties of prostate-specific antigen isoforms in seminal fluid, Prostate 68 (9) (2008) 945–954.
[10] M.T. Peltola, P. Niemela, V. Vaisanen, T. Viitanen, K. Alanen, M. Nurmi, K. Pettersson, Intact and internally cleaved free prostate-specific antigen in patients with prostate cancer with different pathologic stages and grades, Urology 77 (4) (2011) 1009 e1–1009 e8.
[11] G. Untergasser, S. Madersbacher, P. Berger, Benign prostatic hyperplasia: age-related tissue-remodeling, Exp. Gerontol. 40 (3) (2005) 121–128.
[12] H. Lilja, D. Ulmert, A.J. Vickers, Prostate-specific antigen and prostate cancer: prediction, detection and monitoring, Nat. Rev. Cancer 8 (4) (2008) 268–278.
[13] S.P. Balk, Y.J. Ko, G.J. Bubley, Biology of prostate-specific antigen, J. Clin. Oncol. 21 (2) (2003) 383–391.
[14] H. Ozen, S. Sozen, PSA isoforms in prostate cancer detection, Eur. Urol. Suppl. 5 (6) (2006) 495–499.
[15] U.H. Stenman, J. Leinonen, H. Alfthan, S. Rannikko, K. Tuhkanen, O. Alfthan, A complex between prostate-specific antigen and alpha 1-antichymotrypsin is the major form of prostate-specific antigen in serum of patients with prostatic cancer: assay of the complex improves clinical sensitivity for cancer, Cancer Res. (1991) 222–226.
[16] W.M. Zhang, J. Leinonen, N. Kalkkinen, B. Dowell, U.H. Stenman, Purification and characterization of different molecular forms of prostate-specific antigen in human seminal fluid, Clin. Chem. 41 (11) (1995) 1567–1573.
[17] S. Barrabes, N. Farina-Gomez, E. Llop, A. Puerta, J.C. Diez-Masa, A. Perry, R. de Llorens, M. de Frutos, R. Peracaula, Comparative analysis of prostate-specific antigen by two-dimensional gel electrophoresis and capillary electrophoresis, Electrophoresis 38 (3–4) (2017) 408–416.
[18] T. Vermassen, M.M. Speeckaert, N. Lumen, S. Rottey, J.R. Delanghe, Glycosylation of prostate specific antigen and its potential diagnostic applications, Clin. Chim. Acta 413 (19–20) (2012) 1500–1505.
[19] J. Iwakiri, K. Granbois, N. Wehner, H.C. Graves, T. Stamey, An analysis of urinary prostate specific antigen before and after radical prostatectomy: evidence for secretion of prostate specific antigen by the periurethral glands, J. Urol. 149 (4) (1993) 783–786.
[20] J.E. Oesterling, A.H. Tekchandani, S.K. Martin, E.J. Bergstralh, E. Reichstein, E. P. Diamandis, C. Yemoto, T.A. Stamey, The periurethral glands do not significantly influence the serum prostate specific antigen concentration, J. Urol. (1996) 1658–1660.
[21] S. Bolduc, L. Lacombe, A. Naud, M. Gregoire, Y. Fradet, R.R. Tremblay, Urinary PSA: a potential useful marker when serum PSA is between 2.5 ng/mL and 10 ng/mL, Can. Urol. Assoc. J. 1 (4) (2007) 377–381.
[22] I. Sato, M. Sagi, A. Ishiwari, H. Nishijima, E. Ito, T. Mukai, Use of the "SMITEST" PSA card to identify the presence of prostate-specific antigen in semen and male urine, Forensic Sci. Int. 127 (1–2) (2002) 71–74.
[23] E. Scott, J. Munkley, Glycans as biomarkers in prostate cancer, Int. J. Mol. Sci. 20 (6) (2019).
[24] T. Yoneyama, C. Ohyama, S. Hatakeyama, S. Narita, T. Habuchi, T. Koie, K. Mori, K.I. Hidari, M. Yamaguchi, T. Suzuki, Y. Tobisawa, Measurement of aberrant glycosylation of prostate specific antigen can improve specificity in early detection of prostate cancer, Biochem. Biophys. Res. Commun. 448 (4) (2014) 390–396.
[25] N. Leymarie, P.J. Griffin, K. Jonscher, D. Kolarich, R. Orlando, M. McComb, J. Zaia, J. Aguilan, W.R. Alley, F. Altmann, L.E. Ball, L. Basumallick, C.R. Bazemore-Walker, H. Behnken, M.A. Blank, K.J. Brown, S.C. Bunz, C.W. Cairo, J.F. Cipollo, R. Daneshfar, H. Desaire, R.R. Drake, E.P. Go, R. Goldman, C. Gruber, A. Halim, Y. Hathout, P.J. Hensbergen, D.M. Horn, D. Hurum, W. Jabs, G. Larson, M. Ly, B. F. Mann, K. Marx, Y. Mechref, B. Meyer, U. Moginger, C. Neusubeta, J. Nilsson, M. V. Novotny, J.O. Nyalwidhe, N.H. Packer, P. Pompach, B. Reiz, A. Resemann, J. S. Rohrer, A. Ruthenbeck, M. Sanda, J.M. Schulz, U. Schweiger-Hufnagel, C. Sihlbom, E. Song, G.O. Staples, D. Suckau, H. Tang, M. Thaysen-Andersen, R. I. Viner, Y. An, L. Valmu, Y. Wada, M. Watson, M. Windwarder, R. Whittal, M. Wuhrer, Y. Zhu, C. Zou, Interlaboratory study on differential analysis of protein glycosylation by mass spectrometry: the ABRF glycoprotein research multi-institutional study 2012, Mol. Cell. Proteomics 12 (10) (2013) 2935–2951.
[26] N. Mononen, E.H. Seppala, P. Duggal, V. Autio, T. Ikonen, P. Ellonen, J. Saharinen, J. Saarela, M. Vihinen, T.L. Tammela, O. Kallioniemi, J.E. Bailey-Wilson, J. Schleutker, Profiling genetic variation along the androgen biosynthesis and metabolism pathways implicates several single nucleotide polymorphisms and their combinations as prostate cancer risk factors, Cancer Res. 66 (2) (2006) 743–747.
[27] E. Song, Y. Hu, A. Hussein, C.Y. Yu, H. Tang, Y. Mechref, Characterization of the glycosylation site of human PSA prompted by missense mutation using LC-MS/MS, J. Proteome Res. 14 (7) (2015) 2872–2883.
[28] G.S.M. Kammeijer, J. Nouta, J. de la Rosette, T.M. de Reijke, M. Wuhrer, An in-depth glycosylation assay for urinary prostate-specific antigen, Anal. Chem. 90 (7) (2018) 4414–4421.
[29] A. Sarrats, R. Saldova, J. Comet, N. O'Donoghue, R. de Llorens, P.M. Rudd, R. Peracaula, Glycan characterization of PSA 2-DE subforms from serum and seminal plasma, OMICS 14 (4) (2010) 465–474.
[30] M. Santos, C. Ratnayake, D. Horn, B. Karger, A. Ivanov, R. Viner, Separation and Analysis of Intact Prostate Specific Antigen (PSA) and its Proteoforms by CESI-MS Under Native and Denaturing Conditions. https://sciex.com/content/dam/SCIEX/pdf/tech-notes/all/CESI-MS_Intact_Native_Protein_Proteoforms_PSA.pdf, 2015 (Accessed 25th January 2021).
[31] M. Santos, C. Ratnayake, B. Fonslow, A. Guttman, A Covalent, Cationic Polymer Coating Method for the CESI-MS Analysis of Intact Proteins and Polypeptides. htt

ps://sciex.com/content/dam/SCIEX/pdf/tech-notes/all/Covalent-cationic-polymer-coating-method-CESI-MS.pdf, 2015 (Accessed 28th October 2020).
[32] G.S.M. Kammeijer, I. Kohler, B.C. Jansen, P.J. Hensbergen, O.A. Mayboroda, D. Falck, M. Wuhrer, Dopant enriched nitrogen gas combined with sheathless capillary electrophoresis-electrospray ionization-mass spectrometry for improved sensitivity and repeatability in glycopeptide analysis, Anal. Chem. 88 (11) (2016) 5849–5856.
[33] B.C. Jansen, D. Falck, N. de Haan, A.L. Hipgrave Ederveen, G. Razdorov, G. Lauc, M. Wuhrer, LaCyTools: a targeted liquid chromatography-mass spectrometry data processing package for relative quantitation of glycopeptides, J. Proteome Res. 15 (7) (2016) 2198–2210.
[34] J.T. Wu, P. Zhang, T. Wang, L. Wilson, M. Astill, Evaluation of free PSA isoforms, PSA complex formation, and specificity of anti-PSA antibodies by HPLC and PAGE-immunoblotting techniques, J. Clin. Lab. Anal. 9 (1) (1995) 1–14.
[35] H.J. Linton, L.S. Marks, L.S. Millar, C.L. Knott, H.G. Rittenhouse, S.D. Mikolajczyk, Benign prostate-specific antigen (BPSA) in serum is increased in benign prostate disease, Clin. Chem. 49 (2) (2003) 253–259.
[36] T.J. Wang, K.M. Slawin, H.G. Rittenhouse, L.S. Millar, S.D. Mikolajczyk, Benign prostatic hyperplasia-associated prostate-specific antigen (BPSA) shows unique immunoreactivity with anti-PSA monoclonal antibodies, Eur. J. Biochem. 267 (13) (2000) 4040–4045.
[37] S. Gilgunn, P.J. Conroy, R. Saldova, P.M. Rudd, R.J. O'Kennedy, Aberrant PSA glycosylation–a sweet predictor of prostate cancer, Nat. Rev. Urol. 10 (2) (2013) 99–107.
[38] S.D. Mikolajczyk, L.S. Marks, A.W. Partin, H.G. Rittenhouse, Free prostate-specific antigen in serum is becoming more complex, Urology 59 (6) (2002) 797–802.
[39] A. Varki, R. Kannagi, B. Toole, P. Stanley, Glycosylation changes in cancer, in: A. Varki, R.D. Cummings, J.D. Esko, P. Stanley, G.W. Hart, M. Aebi, P.H. Seeberger (Eds.), Essentials of Glycobiology, Cold Spring Harbor, NY, 2015, pp. 597–609.
[40] J.P. Charrier, C. Tournel, S. Michel, S. Comby, C. Jolivet-Reynaud, J. Passagot, P. Dalbon, D. Chautard, M. Jolivet, Differential diagnosis of prostate cancer and benign prostate hyperplasia using two-dimensional electrophoresis, Electrophoresis 22 (9) (2001) 1861–1866.
[41] D. Thakur, T. Rejtar, B.L. Karger, N.J. Washburn, C.J. Bosques, N.S. Gunay, Z. Shriver, G. Venkataraman, Profiling the glycoforms of the intact alpha subunit of recombinant human chorionic gonadotropin by high-resolution capillary electrophoresis-mass spectrometry, Anal. Chem. 81 (21) (2009) 8900–8907.
[42] R. Haselberg, T. De Vijlder, R. Heukers, M.J. Smit, E.P. Romijn, G.W. Somsen, E. Dominguez-Vega, Heterogeneity assessment of antibody-derived therapeutics at the intact and middle-up level by low-flow sheathless capillary electrophoresis-mass spectrometry, Anal. Chim. Acta 1044 (2018) 181–190.
[43] I. van den Broek, W.D. van Dongen, LC-MS-based quantification of intact proteins: perspective for clinical and bioanalytical applications, Bioanalysis 7 (15) (2015) 1943–1958.
[44] X. Qiu, L. Kang, M. Case, N. Weng, W. Jian, Quantitation of intact monoclonal antibody in biological samples: comparison of different data processing strategies, Bioanalysis 10 (13) (2018) 1055–1067.
[45] H. Lilja, J. Oldbring, G. Rannevik, C.B. Laurell, Seminal vesicle-secreted proteins and their reactions during gelation and liquefaction of human semen, J. Clin. Invest. 80 (2) (1987) 281–285.
[46] T. Vermassen, C. Van Praet, D. Vanderschaeghe, T. Maenhout, N. Lumen, N. Callewaert, P. Hoebeke, S. Van Belle, S. Rottey, J. Delanghe, Capillary electrophoresis of urinary prostate glycoproteins assists in the diagnosis of prostate cancer, Electrophoresis 35 (7) (2014) 1017–1024.
[47] A.B. Moran, E. Dominguez-Vega, J. Nouta, T. Pongracz, d.T.M. Reijke, M. Wuhrer, G.S.M. Lageveen-Kammeijer, Profiling the Proteoforms of Urinary Prostate-Specific Antigen by Capillary Electrophoresis – Mass Spectrometry - Data Set, MassIVE (Ed.), 2021.